axioms

IMPACT FACTOR 1.9

Article

The Golden Ratio Family of Extremal Kerr-Newman Black Holes and Its Implications for the Cosmological Constant

Giorgio Sonnino and Pasquale Nardone

Special Issue
Advances in Differential Geometry and Mathematical Physics

Edited by
Dr. David D. McNutt

MDPI

https://doi.org/10.3390/axioms13120862

axioms

MDPI

Article

The Golden Ratio Family of Extremal Kerr-Newman Black Holes and Its Implications for the Cosmological Constant

Giorgio Sonnino * and Pasquale Nardone

Department of Physics, Université Libre de Bruxelles (U.L.B.), Campus de la Plaine C.P. 224 - Bvd du Triomphe, 1050 Brussels, Belgium; pasquale.nardone@ulb.be

* Correspondence: giorgio.sonnino@ulb.be

Abstract: This work explores the geometry of extremal Kerr-Newman black holes by analyzing their mass/energy relationships and the conditions ensuring black hole existence. Using differential geometry in E^3, we examine the topology of the event horizon surface and identify two distinct families of extremal black holes, each defined by unique proportionalities between their core parameters: mass (m), charge (Q), angular momentum (L), and the irreducible mass (m_{ir}). In the first family, these parameters are proportionally related to the irreducible mass by irrational numbers, with a characteristic flat Gaussian curvature at the poles. In the second family, we uncover a more intriguing structure where m, Q, and L are connected to m_{ir} through coefficients involving the golden ratio $-\phi_-$. Within this family lies a unique black hole whose physical parameters converge on the golden ratio, including the irreducible mass and polar Gauss curvature. This black hole represents the highest symmetry achievable within the constraints of the Kerr-Newman metric. This remarkable symmetry invites further speculation about its implications, such as the potential determination of the dark energy density parameter Ω_Λ for Kerr-Newman-de Sitter black holes. Additionally, we compute the maximum energy that can be extracted through reversible transformations. We have determined that the second, golden-ratio-linked family allows for a greater energy yield than the first.

Keywords: black holes; differential geometry; relativity and gravitational theory; astronomy and astrophysics; Kerr–Newman metric

MSC: 83F05; 85A40; 54A99; 53A05; 53B25; 53C80

Citation: Sonnino, G.; Nardone, P. The Golden Ratio Family of Extremal Kerr-Newman Black Holes and Its Implications for the Cosmological Constant. *Axioms* **2024**, *13*, 862. https://doi.org/10.3390/axioms13120862

Academic Editor: David D. McNutt

Received: 31 October 2024
Revised: 29 November 2024
Accepted: 7 December 2024
Published: 10 December 2024

1. Introduction

The Kerr-Newman black hole is a solution to the equations of general relativity that describe a rotating and charged black hole [1,2]. It incorporates both the effects of angular momentum (spin) and electric charge, making it a more complex and realistic model than the non-rotating, uncharged Schwarzschild black hole or the Reissner-Nordström black hole (which has charge but no spin). While real black holes are not expected to carry large electric charges, the study of charged black holes can provide insights into cosmological scenarios where charged black holes may have formed in the early universe. These scenarios could involve interactions with electrically charged particles during the universe's early stages. Many astrophysical objects, such as accreting black holes in binary systems or active galactic nuclei, may possess both angular momentum and electric charge. The Kerr-Newman solution helps physicists and astronomers understand the effects of rotation and charge on the behavior of these objects, including how they emit radiation, affect their surroundings, and influence their accretion processes. Additionally, studying the Kerr-Newman solution provides opportunities to test the predictions of general relativity under more complex conditions. The curvature of spacetime around a rotating charged black hole is different from that of simpler black holes, and studying these differences allows for tests of the theory's predictions in extreme scenarios. Investigating the extreme Kerr-Newman

black hole is important to explore the relationships between gravity and thermodynamics and contribute to our broader understanding of fundamental physics. For example, exploring Kerr-Newman black holes in extremal conditions provides deeper insights into the Hawking radiation mechanism (ref. to [3], for instance). The description of black holes is notably simplified by adopting the validity of the so-called *no-hair theorem* [4–6]. The no-hair theorem is a concept in theoretical physics that suggests that the observable properties of a black hole, such as its mass (m), charge (Q), and angular momentum L, are the only relevant characteristics that can be determined from the outside. In other words, the complex details of the matter that formed the black hole are unimportant for describing its long-term behavior. Studies involving black hole mergers and gravitational wave detections have supported the no-hair theorem in recent years. Nonetheless, exploring black holes and their properties remains an active area of research, and our understanding of these enigmatic objects continues to evolve. Recent investigations showed that studying extreme black holes may shed some light on their feature properties outside of the three classical black hole traits of mass, charge, and spin [7]. While the no-hair theorem asserts that black holes are fully described by just three observable quantities-mass, charge, and spin-the study of the linear stability of Schwarzschild singularities looks into the internal dynamics and stability of black holes under perturbations. This kind of analysis can reveal deeper structural and stability-related properties that are not captured by the no-hair description alone. In this paper, we investigate two relevant extremal, charged, rotating families of black holes that are determined by examining the geometric version of the mass/energy formula combined with the equation for the existence of extremal Kerr–Newman black holes. The topology of event horizon surfaces will be studied using the tools provided by differential geometry. When a black hole rotates, its surface deforms; there is the characteristic flattening of the poles and lengthening of the equatorial circumference. The first family of black holes analyzed by us corresponds to the extremal Kerr-Newman black holes where the Gaussian curvatures of the horizon surface vanish at the poles, and m, Q, and L are connected with the irreducible mass m_{ir} by irrational numbers. The second family is much more spectacular and intriguing, and to the best of our knowledge, it is the first time that it has been reported in the literature. In the second family, the physical quantities of the black holes—m, Q, and L—are connected to m_{ir} through coefficients involving the golden ratio $-\phi_- = (\sqrt{5}-1)/2 \simeq 0.618$. Belonging to this family, there is a special extremal black hole that satisfies the Pythagorean relations among the fundamental forms at the umbilic points. For this special black hole, all fundamental physical quantities-mass, charge, angular momentum, and irreducible mass-align with the golden ratio. This exceptional black hole represents the pinnacle of symmetry achievable within the Kerr-Newman framework. As we shall discuss in Section 6, this profound alignment, compatible with the constraints of the Kerr-Newman metric, hints at a unique state of equilibrium that may even offer a pathway to determine the dark energy density parameter Ω_Λ for black holes in the Kerr-Newman-de Sitter geometry. Typically, black holes are described by the Kerr-Newman solution, which encapsulates the complex interplay of rotation and charge in these cosmic entities. In the case of an extremal black hole, this configuration is pushed to the edge, with mass, charge, and angular momentum in precise balance, barely preventing a transition to a naked singularity. The alignment of these parameters according to the golden ratio could signal an ultimate equilibrium, where this extraordinary symmetry minimizes disturbances and optimizes stability. Remarkably, the golden ratio, $-\phi_-$, has long been associated with stable, self-organizing systems in nature [8]. For a black hole, this could imply a configuration in which irreducible mass, extractible energy, charge, and angular momentum are proportionate and arranged in a way that could form a highly resilient system resistant to external perturbations. The thermodynamic stability of such a black hole could be assessed through quantities like specific heat and the principles of black hole mechanics, particularly the second law. If these quantities are also aligned with the golden ratio, it would suggest a state where fluctuations in entropy and temperature are minimal-signifying a black hole in a state of profound thermodynamic stability. The notion

of a black hole reaching a *golden ratio state*, where fundamental properties are in perfect resonance, implies an ideal configuration that could act as an "attractor" in the evolutionary trajectory of black holes [9,10]. In the broader view of dynamic systems, an attractor is a set of values toward which a system naturally evolves, regardless of its initial conditions. Suppose black holes are indeed drawn toward this golden ratio alignment. In that case, it suggests that they could inherently evolve toward this ultimate stable state—analogous to how other natural systems seek states of minimal energy and maximal stability.

The structure of this work is as follows. Section 2 introduces extreme black holes within the Kerr-Newman geometry framework, establishing foundational concepts. Section 3 identifies two distinct families of extremal Kerr-Newman black holes. As demonstrated in Appendix A, these classifications arise naturally from a geometric interpretation of the mass/energy relation and the inequality that ensures the existence of such black holes. Section 4 positions and describes these two families within the Christodoulou diagram, offering insights into their distinct properties. Section 5 delves into the topology of these extremal black holes, employing differential geometry to analyze their structural characteristics. In Section 6, we briefly outline the approach for calculating the dark energy density parameter, Ω_λ, through the unique properties of the extremal Kerr-Newman black hole with golden ratio symmetry within the Kerr-Newman-de Sitter geometry. Section 7 calculates the energy that can be reversibly extracted from these extremal Kerr-Newman black holes. Section 8 provides concluding remarks, summarizing the implications of our findings. The appendices contain detailed proofs of the key theorems and derivations. Specifically, Appendix A revisits the geometric form of the mass/energy formula and the existence equation for extremal Kerr-Newman black holes. Appendix B presents the derivations of the first and second fundamental forms and the equation for the umbilic points. Appendix C provides the solution to the equation of the Pythagorean fundamental forms.

2. Extremal Black Holes in the Kerr–Newman Geometry

In the Kerr-Newman geometry, the outer horizon is located at [4]

$$r_+ = m + \sqrt{m^2 - Q^2 - a^2} \tag{1}$$

where m is the mass of the black hole, Q is the charge, and $a = L/m$ is the angular momentum per unit mass. In Equation (1), we use Planck's unit system, where the five universal physical constants, i.e., the speed of light c, the universal gravitational constant G, the reduced Planck's constant $\hbar$, Boltzmann's constant k_B, and the vacuum permittivity ε_0 take on the numerical value of 1 when expressed in terms of these units the modern values for Planck's original choice of quantities are as follows: *Planck's length* = $\sqrt{\hbar G/c^3}$, *Planck's mass* = $\sqrt{\hbar c/G}$, *Planck's angular momentum* = $\hbar$, *Planck's temperature* = $\sqrt{\hbar c^5/(Gk_B^2)}$, *Planck's energy* = $\sqrt{\hbar c^5/G}$, and *Planck's charge* = $\sqrt{4\pi\varepsilon_0\hbar c} = e/\sqrt{\alpha}$, with e and α denoting the electric charge and the fine-structure constant, respectively). Unless otherwise indicated, Planck's unit system will be adopted in the sequel. The Kerr–Newman black hole exists if we have the following:

$$m^2 \geq Q^2 + a^2 \tag{2}$$

Any collapsing body that violates this constraint, centrifugal forces, and/or electrostatic repulsion will halt the collapse before a size $\sim m$ is reached. Notice that due to the no-hair theorem, all information about the matter in the hole is missing for an outside observer except the total mass, angular momentum, and charge of the black hole. Equation (1) can be rewritten in an alternative form by expressing the mass/energy formula of a Kerr–Newman black hole m in terms of the irreducible mass m_{ir} (as well as a function of the charge Q and of the angular momentum L) [11–14]:

$$m^2 = \left(m_{ir} + \frac{Q^2}{4m_{ir}}\right)^2 + \frac{L^2}{4m_{ir}^2} \tag{3}$$

where the irreducible mass is defined as follows:

$$m_{ir} \equiv \frac{1}{2}\sqrt{r_+^2 + a^2} \tag{4}$$

In this form, the Kerr–Newman black hole exists if we have the following [12]:

$$\frac{L^2}{4m_{ir}^4} + \frac{Q^4}{16m_{ir}^4} \leq 1 \tag{5}$$

The surface area of the event A (i.e., the horizon) is located at the $r_h = gravitational\ radius$ [4]. So, we have the following:

$$A = 4\pi r_h^2 \tag{6}$$

Only the region on and outside the black hole's surface, $r \geq 2m_{ir}$, is relevant to external observers [12]. Events inside the horizon can never influence the exterior. The horizon is related to the irreducible mass according to the equation $r_h = 2m_{ir}$ and the expression of the surface area of the event reads as follows [12]:

$$A = 16\pi m_{ir}^2 \quad \text{so} \quad \frac{A}{4\pi} = r_+^2 + a^2 = 2m(m + \sqrt{m^2 - Q^2 - a^2}) - Q^2 \tag{7}$$

- **The extreme Kerr–Newman black holes.**

  The extremal black hole is described by the following equations:

$$\begin{aligned} m^2 &= \left(m_{ir} + \frac{Q^2}{4m_{ir}}\right)^2 + \frac{L^2}{4m_{ir}^2} \\ \frac{L^2}{4m_{ir}^4} &+ \frac{Q^4}{16m_{ir}^4} = 1 \end{aligned} \tag{8}$$

Equation (6) can be brought in the following form:

$$\begin{aligned} (\sqrt{2}m_{ir})^2 + \left(\frac{Q}{\sqrt{2}}\right)^2 &= m^2 \\ a^2 + \left(\frac{Q}{\sqrt{2}}\right)^2 &= (\sqrt{2}m_{ir})^2 \end{aligned} \tag{9}$$

Equation (9) are the equations for an extreme Kerr–Newman black hole. Note that substituting the expression for $2m_{ir}$ given by the first equation of System (9) into the second equation of System (9) we re-obtain the following:

$$a^2 + Q^2 = m^2 \tag{10}$$

Substituting the expression for $Q/\sqrt{2}$ given by the first equation of System (9) into the second equation of System (9) we obtain the following:

$$a^2 + m^2 = (2m_{ir})^2 \tag{11}$$

So, $m_{ir} \leq m \leq 2m_{ir}$; the minimum value of energy m corresponds to a Schwarzschild black hole ($L = 0$ and $Q = 0$) and its maximum value to the extreme Reissner–Nordström

black hole ($L = 0$). It is convenient to remove numbers like 2 or $\sqrt{2}$ and rewrite the equations for the extreme Kerr–Newman black holes in terms of the following *scaled quantities*:

$$\begin{aligned} \bar{L} &\equiv 2L \\ \bar{m} &\equiv \sqrt{2}m \\ \eta &\equiv 2m_{ir} \end{aligned} \tag{12}$$

In the literature, parameter η is called the *scale parameter* [14,15]. In terms of variables $\bar{L}$, $\bar{m}$, and η, the equations for the extreme Kerr–Newman black holes notably simplify the following:

$$\begin{aligned} \eta^2 + Q^2 &= \bar{m}^2 \\ \bar{a}^2 + Q^2 &= \eta^2 \end{aligned} \tag{13}$$

where $\bar{a} = \bar{L}/\bar{m} = \sqrt{2}\,a$. In the appendix, we can verify that Equations (9)–(11) are equivalent, from a geometrical point of view to four right triangles interconnected with each other (see the Annex in Figure A1).

3. Two Meaningful Families of Extremal Kerr–Newman Black Holes

Two very special extremal black holes deserve attention. We denote these as case (i) and case (ii), satisfying the following special conditions [16]:

3.1. Case (i)

$$|Q| = \frac{1}{\sqrt{2}}\eta \tag{14}$$

In this case, from System (9), we obtain the following:

$$\begin{aligned} \bar{m} &= \sqrt{\frac{3}{2}}\eta \\ |Q| &= \frac{1}{\sqrt{2}}\eta \\ |\bar{L}| &= \frac{\sqrt{3}}{2}\eta^2 \end{aligned} \tag{15}$$

From the geometrical point of view, Equation (14) corresponds to the particular configuration, where the triangle ABC coincides with triangle ACE (see Appendix Figure A2).

3.2. Case (ii)

$$|\bar{L}| = \eta|Q| \tag{16}$$

From the geometrical point of view, Equation (16) corresponds to the particular configuration where the catheter BD of the right triangle ADB coincides exactly with the height of the triangle ABC relative to the base AC (see Figure A3 in the appendix). In this case, we can see that the charge $|Q| = |L|/m_{ir}$ turns out to be a combination of the angular momentum L with the irreducible mass m_{ir}, which is an intrinsic quantity of the Kerr-Newman metric. By plugging condition (16) into Equation (13), we obtain the following:

$$\begin{aligned} \bar{m} &= (-\phi_-)^{-1/2}\eta \\ |Q| &= (-\phi_-)^{1/2}\eta \\ |\bar{L}| &= (-\phi_-)^{1/2}\eta^2 \end{aligned} \tag{17}$$

where ϕ_- is one of the solutions to the golden ratio equation, as follows:

$$\phi^2 - \phi - 1 = 0 \tag{18}$$

i.e.,

$$\phi_- = \frac{1-\sqrt{5}}{2} \tag{19}$$

Note that the other solution ϕ_+ of the golden ratio equation (Equation (A5)) is linked to ϕ_- by the relation $\phi_+ = (-\phi_-)^{-1}$. Equation (17) states that there exists a whole family of charged rotating extremal black holes in which the fundamental quantities are incommensurate with its irreducible mass and the irrational constants depend solely on the golden ratio. In the next section, we shall analyze the extreme black holes (15) and (17) in Christodoulou's diagram.

4. Two Extremal Kerr-Newman Black Holes in the Christodoulou Diagram

4.1. The Christodoulou Diagram

Christodoulou's diagram shows the contours m/m_{ir} in the plane scaled angular momentum L/m_{ir}^2 versus scaled charge Q/m_{ir} [17]. Black holes exist only in the interior of the region $a^2 + Q^2 \leq m^2$. The Christodoulou diagram is easily obtained by introducing the following scaled variables:

$$\begin{aligned} x &= \frac{Q}{\eta} \\ y &= \frac{\bar{L}}{\eta^2} \\ z &= \sqrt{2}\frac{\bar{m}}{\eta} = \frac{m}{m_{ir}} \end{aligned} \tag{20}$$

In the new variables, the equations for the Kerr–Newman black holes (3) and (5) read as follows:

$$z^2 - \left(1 + x^2\right)^2 - y^2 = 0 \qquad \text{with} \qquad x^4 + y^2 \leq 1 \tag{21}$$

The extreme black holes satisfy the equation $x^4 + y^2 = 1$. Accordingly, one finds the x, y, and z range for the family of black holes associated with the given η:

$$-1 \leq x \leq 1 \quad ; \quad -1 \leq y \leq 1 \quad \text{and} \quad 1 \leq z \leq 2 \tag{22}$$

Figure 1 shows the behavior of the mass/energy formula for a Kerr–Newman black hole. These black holes exist in the ranges (22).

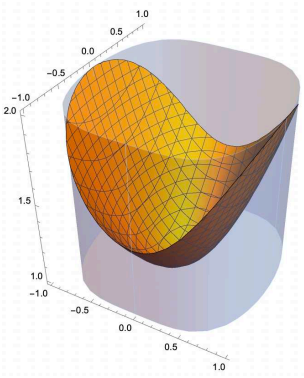

Figure 1. Mass/energy formula for the Kerr–Newman black holes (the orange surface). These black holes exist only in the range of $x^4 + y^2 \leq 1$ (the gray zone).

Equations (15) and (17) refer to extreme black holes. Indeed, for the extreme black hole (15), with a positive charge and angular momentum, we obtain the following:

$$\begin{aligned} x &= \frac{|Q|}{\eta} = \frac{1}{\sqrt{2}} = 0.707107 \\ y &= \frac{|\bar{L}|}{\eta^2} = \frac{\sqrt{3}}{2} = 0.866025 \quad \text{so} \\ x^4 + y^2 &= \frac{1}{4} + \frac{3}{4} = 1 \end{aligned} \tag{23}$$

in agreement with Equation (10). For the extreme black hole (17), with a positive charge and angular momentum, we obtain the following:

$$\begin{aligned} x &= \frac{|Q|}{\eta} = (-\phi_-)^{1/2} = \frac{\sqrt{\sqrt{5}-1}}{\sqrt{2}} = 0.786151 \\ y &= \frac{|\bar{L}|}{\eta^2} = (-\phi_-)^{1/2} = \frac{\sqrt{\sqrt{5}-1}}{\sqrt{2}} = 0.786151 \qquad \text{so} \\ x^4 + y^2 &= \phi_-^2 - \phi_- = 1 + \phi_- - \phi_- = 1 \end{aligned} \tag{24}$$

where we take into account the identity $\phi_-^2 = 1 + \phi_-$.

4.2. Location of the Extremal Black Holes (15) and (17) in Christodoulou's Diagram

Case (i)

$$\begin{aligned} &\text{Contour : } z_c = \sqrt{3} = 1.73205 \\ &\text{Coordinate of the black hole : } \{x, y\} = \left\{1/\sqrt{2}, \sqrt{3}/2\right\} \end{aligned} \tag{25}$$

Case (ii)

$$\begin{aligned} &\text{Contour : } z_c = \frac{\sqrt{2}}{\sqrt{-\phi_-}} = 1.79891 \\ &\text{Coordinate of the black hole : } \{x, y\} = \left\{(-\phi_-)^{1/2}, (-\phi_-)^{1/2}\right\} \end{aligned} \tag{26}$$

Figures 2 and 3 show the locations of the two extreme black holes (15) and (17), respectively, in the scaled Christodoulou diagram.

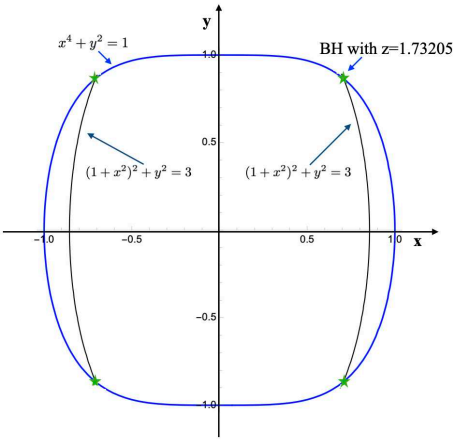

Figure 2. Scaled Christodoulou's diagram. Contours of constant $z = m/m_{ir}$ are depicted in the x-y plane. Black holes can exist only in the interior of the region $x^4 + y^2 \leq 1$. Black holes in the blue contour are the extreme black holes. The green stars correspond to the extreme black holes (15).

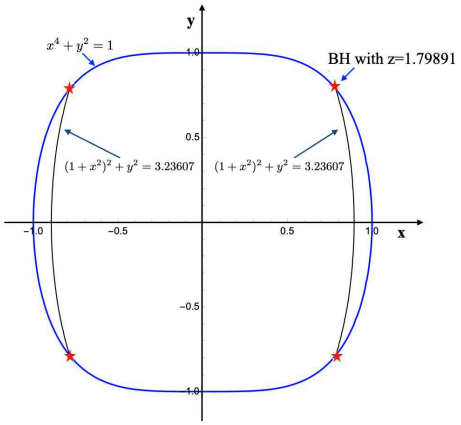

Figure 3. Scaled Christodoulou's diagram. Contours of constant $z = m/m_{ir}$ are depicted in the x-y plane. The extreme black holes are located in the blue curve $x^4 + y^2 \leq 1$. The red stars refer to the extreme black holes (17). Note that black holes marked by red stars are the only extreme Kerr–Newman black holes that satisfy the symmetry $|y| \leftrightarrow |x|$.

Notice that the coordinates of the other six extreme black holes, indicated by the green and red stars, can be easily obtained by setting $z_c = 1.73205$, for case (i), and $z_c = 1.79891$, for case (ii), in Equation (21), respectively, and solving the equations for variables x and y.

4.3. Symmetries

As we can see, the plots of the Christodoulou diagram are symmetric concerning the following transformations $\{x, y\} \to \{-x, y\}$, i.e., symmetry concerning the reflection about the L-axis (the *Kerr axis*), $\{x, y\} \to \{x, -y\}$, i.e., symmetry for the reflection about the Q-axis (the *Reissner-Nordström axis*), and $\{x, y\} \to \{-x, -y\}$, i.e., symmetry concerning the origin of the axes $(Q, L) = (0, 0)$ (the *Schwarzschild point*). We can easily verify that the black holes (17) (indicated by red stars in this diagram) are the only ones invariant under the exchange of $|y|$ with $|x|$ (and vice-versa). Indeed, extreme Kerr-Newman black holes satisfy the following equation:

$$x^4 + y^2 - 1 = 0 \tag{27}$$

We are looking for extreme black holes that are invariant concerning the exchange of $|y|$ with $|x|$, and vice-versa. This symmetry requires that x satisfies equation [16], as follows:

$$x^4 + x^2 - 1 = 0 \tag{28}$$

Equation (28) admits only one positive solution x^2 given by the following:

$$x^2 = -\phi_- \qquad \text{or} \qquad |x| = (-\phi_-)^{1/2} = |y| \tag{29}$$

Plugging these solutions into the mass/energy formula (21), we obtain the value of z as follows:

$$z = \sqrt{2\phi_+} = \frac{\sqrt{2}}{\sqrt{-\phi_-}} \tag{30}$$

in agreement with Equations (24) and (26). In short, the extreme Kerr-Newman black holes marked by red stars are quite peculiar since they belong to the family of black holes located on the bisectors of the Christodoulou diagram. The next section is devoted to the study of the geometrical properties of the two extreme black holes (i) and (ii).

5. Study of the Surface Geometry of the Extremal Black Holes

To visualize the intrinsic geometry of a black hole, we embed the surface isometrically in the Euclidean 3D space E^3 [15]. First, it is convenient to introduce a metric function $h(\mu)$ defined as follows:

$$h(\mu) = (1-\mu^2)[1-\beta^2(1-\mu^2)]^{-1} \qquad \text{where} \quad \beta = \frac{a}{\eta} \tag{31}$$

In the literature, the parameter β is called a distortion parameter. In Kerr–Newman geometry, the metric is written in a standard form, as follows [1,15]:

$$ds^2 = \eta^2(h(\mu)^{-1}d\mu^2 + h(\mu)d\psi^2) \quad \text{with} \quad -1 \le \mu \le 1 \ , \ 0 \le \psi \le 2\pi \tag{32}$$

The values $\mu = \pm 1$ correspond to the poles. The equator corresponds to the value $\mu = 0$. The procedure for investigating an arbitrary surface of revolution in E^3 is standard. As a curve $\mathcal{C}$ in the xz-plane $\mathrm{x} = f(\nu)$, $\mathrm{z} = g(\nu)$ revolves around the z-axis; it generates a surface of revolution $\mathcal{S}$. The curves $\mathcal{C}$ in different rotated positions are the meridians of $\mathcal{S}$. In contrast, the circles generated by each point on $\mathcal{C}$ are the parallels of $\mathcal{S}$ (see Figure 4).

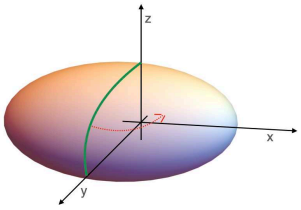

Figure 4. The horizon surface of a black hole, when embedded in Euclidean 3-space, forms a surface of revolution.

If we denote the rotation angle in the xy-plane as θ, the surface of revolution can be parametrized as follows:

$$(\mathrm{x}, \mathrm{y}, \mathrm{z}) = (f(\nu)\cos\theta, f(\nu)\sin\theta, g(\nu)) \tag{33}$$

By equating the 2-metric resulting from (33), we have the following:

$$ds^2 = (f'^2 + g'^2)d\nu^2 + f^2 d\theta^2 \tag{34}$$

with metric (32), we obtain $\nu = \mu$, $\theta = \psi$, and

$$f(\mu) = \eta h^{1/2} \qquad ; \qquad g'(\mu) = h^{-1/2}\left(1 - \frac{1}{4}h'^2\right)^{1/2} \tag{35}$$

where prime stands for the derivative with respect to μ. The first fundamental form $\mathcal{I}$ and the second fundamental form $\mathcal{II}$ of surface (33) read as follows (see the appendix):

$$\begin{aligned} \mathcal{I} &= \begin{pmatrix} E & 0 \\ 0 & G \end{pmatrix} = \eta \begin{pmatrix} h^{-1} & 0 \\ 0 & h \end{pmatrix} \\ \mathcal{II} &= \begin{pmatrix} L & 0 \\ 0 & N \end{pmatrix} = \eta^{-2} \begin{pmatrix} f(g''f' - g'f'') & 0 \\ 0 & f^2 g' \end{pmatrix} \end{aligned} \tag{36}$$

So, the Gaussian curvature K_G for a metric of the above form is given by the following: [18,19]

$$K_G = \frac{LN}{(EG)^2} = -\frac{1}{2}h''\eta^{-2} = \eta^{-2}\left(1-\beta^2\left(1+3\mu^2\right)\right)\left(1-\beta^2\left(1-\mu^2\right)\right)^{-3} \tag{37}$$

It is useful to recall that the range of charge and total mass/energy for the family of Kerr–Newman black holes associated with the given parameters β and η are [15]:

$$\begin{aligned} 0 \leq Q &\leq \eta\left(1-2\beta^2\right)^{1/2} \\ \frac{1}{2}\eta\left(1-\beta^2\right)^{-1/2} &\leq m \leq \eta(1-\beta)^2 \end{aligned} \tag{38}$$

5.1. Case (i)

In this particular case, we find that the value of the *distortion parameter* β is $1/2$. For this particular value of β, the Kerr metrics break into two classes separated by $\beta = 1/2$ [15]. For $\beta < 1/2$, the horizon of black holes resembles oblately deformed spheres when embedded in Euclidean 3-space, exhibiting uniformly positive Gaussian curvature. For $\beta > 1/2$, there are regions of negative Gaussian curvature both on and around the axis of symmetry. In this case, the surface most resembles a hybrid sphere and pseudo-sphere. When $\beta = 1/2$ (i.e., $a = m_{ir}$), at the poles ($\mu = \pm 1$), the curvature of the event horizon surface becomes flat as the Gaussian curvature K_G vanishes at these points. For an uncharged rotating Kerr black hole, it can be easily verified that this condition is met when $a = \sqrt{3}/2m$. Beyond the value $\beta = 1/2$, a global embedding in the Euclidean 3-space is impossible. To summarize, the black hole corresponding to configuration (15) is an extreme Kerr–Newman black hole where the curvature at the poles becomes flat.

5.2. Case (ii)

For the black hole (17), we obtain the following:

$$\beta = \frac{1}{\sqrt{2}}(-\phi_-) = 0.437016 \tag{39}$$

Since the value of β is less than $1/2$, the black hole horizon (17) is a surface of revolution that can be embedded in the Euclidean 3-space [15]. To gain more insight into the true intrinsic nature of the surface, one must look locally. This task will be accomplished in the following subsections.

5.2.1. Umbilic Points

An *umbilic* is a point on a surface where all normal curvatures are equal in all directions and, hence, principal directions are indeterminate. Thus, the orthogonal net of lines of curvature becomes singular at an umbilic. Spheres and planes are the only surfaces whose points are umbilical. A non-flat umbilic occurs at an elliptic point where the principal forms $\mathcal{I}$ and $\mathcal{II}$ are proportional. So, at the umbilic, we have the following relation [20,21]:

$$\begin{aligned} &Ł = \kappa E \\ &G = \kappa N \\ &F = \kappa M \qquad \text{with} \qquad \kappa = constant \end{aligned} \tag{40}$$

It can be easily verified that, for metric (32), we have $F = M = 0$. In the appendix, we show that for metric (32) the umbilic should satisfy equation [16], as follows:

$$(1-\mu^2)\left(1-\beta^2\left(1+3\mu^2\right)\right) - \left(1-\beta^2\left(1-\mu^2\right)\right)^4 + \mu^2 = 0 \tag{41}$$

When the limit $\beta = 1/\sqrt{2}$ is exceeded, a naked singularity occurs [15]. We can verify that Equation (41) admits only one solution in the range $0 \leq \beta \leq 1/\sqrt{2}$ corresponding to $\mu = \pm 1$. This solution is satisfied for all values of parameter β. In other words, for metric (32), the umbilic points are located at the poles (see Figure 5).

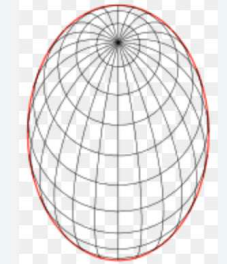

Figure 5. Umbilic points. For metric (32), the umbilic points are located at the poles.

5.2.2. The Pythagorean Fundamental Form Relation

In the appendix, we prove the following result: Consider the Kerr–Newman black hole surface with metric (32) immersed into E^3, satisfying the *Pythagorean fundamental form relation* at the umbilic points as follows:

$$\mathcal{I}^2 + \mathcal{II}^2 = \mathcal{III}^2 \tag{42}$$

with $\mathcal{I}$, $\mathcal{II}$, and $\mathcal{III}$ denoting the matrices corresponding to the first, second, and third fundamental forms of the surface, respectively. Then, in the Planck unit system, at the umbilic points, the *mean curvature of the surface* H and the *Gauss curvature of the surface* K_G are, respectively, given by the following [16]:

$$\begin{aligned} H &= (\phi_+)^{1/2} = (-\phi_-)^{-1/2} \\ K_G &= \phi_+ = (-\phi_-)^{-1} \end{aligned} \tag{43}$$

This result is in line with the result shown in [22]. Furthermore, the value of the *scale parameter* η is as follows:

$$\eta = -\phi_- \tag{44}$$

We recall that the third fundamental form of the surface is the square of the differential of the unit normal vector surface at the point of a surface. The linear dependence relates the three fundamental forms as follows:

$$K_G \cdot \mathcal{I} - 2H \cdot \mathcal{II} + \mathcal{III} = 0 \tag{45}$$

To summarize, the main result of our analysis is as follows:
The extreme Kerr–Newman black hole, i.e.,

$$\begin{aligned} \bar{m} &= (-\phi_-)^{1/2} \\ |Q| &= (-\phi_-)^{3/2} \\ |\bar{L}| &= (-\phi_-)^{5/2} \end{aligned} \tag{46}$$

satisfying the Pythagorean fundamental form relation at the umbilic points, is the unique black hole where the *scale parameter* η is equal to a golden ratio (recall that we have adopted Planck's unit system). Recall that a sphere of surface area $4\pi r_G^2$ has $K_G = 1/r_G^2$, which is constant and positive. For this particular black hole, at the pole, the Gaussian curvature (in Planck's unit system) is as follows:

$$K_G = \frac{1}{r_G^2} \qquad \text{where} \qquad r_G = (-\phi_-)^{1/2} \tag{47}$$

Hence, *the surface of the extreme Kerr-Newman black hole (17) that satisfies the Pythagorean fundamental form relation at the umbilic points is locally metrically equivalent to a 2-sphere at these points, with the radius of curvature equal to the square root of the golden ratio.* Figure 6 (in the Christodoulou diagram) shows the family to which the *extremal Kerr-Newman black holes with*

golden symmetry (EKNBHGRS) belong (see the four red stars inside a circle). Notice that we have four extreme black holes due to the invariances $Q \to -Q$ and $L \to -L$. Since Christodoulou diagrams are parametric, it is possible to visualize only families of black holes but not individual ones. Extremal Kerr-Newman black holes that satisfy the mass/energy formula lie on the surface shown in Figure 7. Notice that for extremal black holes, the charge Q and angular momentum L are interdependent, leaving only one as an independent variable. The blue dot represents the extremal Kerr-Newman black hole with golden symmetry within the family positioned in the first quadrant of the Christodoulou diagram.

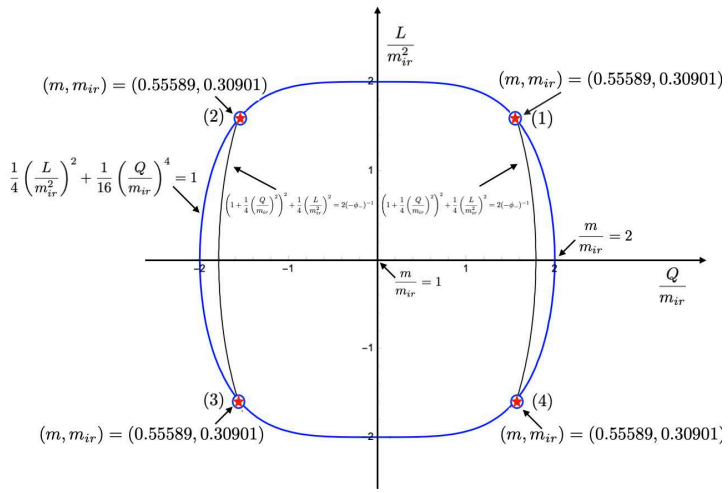

Figure 6. The red stars inside a circle shown in the Christodoulou diagram indicate the locations of the families of extremal black holes to which the Kerr-Newman black holes with golden symmetry (EKNBHGRS) belong. The value of the contour level is given by $m/m_{ir} = \sqrt{2}(-\phi_-)$. Extremal Kerr-Newman black holes with golden symmetry are situated at the intersections of these contour lines with the extremal curve. The mass and irreducible mass of the extremal Kerr-Newman black hole with golden ratio symmetry (EKNBHGRS) are $(m, m_{ir}) = (0.55589, 0.30901)$.

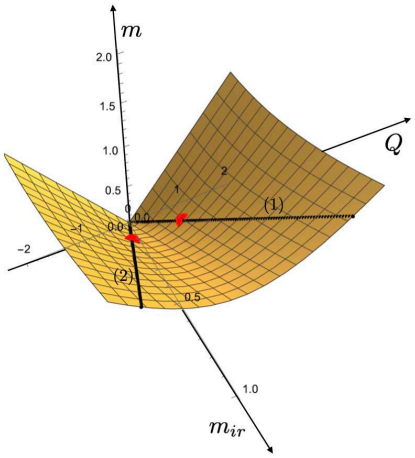

Figure 7. The surface is the loci of extremal Kerr-Newman black holes that satisfy the mass/energy formula. The red points on this surface, with coordinates $(m_{ir}, Q, m) = (-1/2\phi_-, (-\phi_-)^{-3/2}, 1/\sqrt{2}(-\phi_-)^{1/2})$ and $(m_{ir}, Q, m) = (-1/2\phi_-, -(-\phi_-)^{-3/2}, 1/\sqrt{2}(-\phi_-)^{1/2})$, locate the EKNBHGRS in the first and the second quadrants of the Christodoulou diagram, respectively (see the red stars (1) and (2) in Figure 6). The black lines on the surface are the loci of extreme Kerr-Newman black holes, where the mass, charge, and angular momentum are proportional to the irreducible mass, with proportionality coefficients corresponding to the golden ratio. Notice that for these extreme black holes, the angular momentum L is not an independent variable as $|L| = m_{ir}|Q|$. So, the EKNBHGRS (3) and (4) in Figure 6 have, respectively, the same coordinate of (1) and (2), but with opposite values of angular momentum.

5.3. Discussion

The Pythagorean relation holds exclusively at the umbilical points, signifying that it is a local property of the event surface rather than a global one - except in the case of the Schwarzschild black hole, where it applies globally. Furthermore, the use of the Smarr procedure and the Smarr formula in our calculations is a significant step toward establishing the coordinate-independent nature of the derived properties of EKNBHGRS. This becomes clear from the following:

Smarr formula and coordinate independence.

The Smarr formula is a geometric and thermodynamic relationship for black holes that links their mass m, charge Q, angular momentum L, and surface area (or irreducible mass m_{ir}). It is derived from the underlying Einstein field equations and relies on global spacetime properties rather than any specific coordinate system. By using the Smarr metric and applying the Smarr procedure we have the following:

(i) Our calculations are rooted in the intrinsic geometry of the Kerr–Newman black hole.

(ii) The quantities m, Q, L, and m_{ir} are scalar invariants, meaning their definitions are invariant under coordinate transformations. Since the Pythagorean relation emerges directly from these invariants (e.g., through the mass/energy formula), the relation itself should also hold independently of the chosen coordinate system.

Embedding and isometry in E^3.

The isometric embedding of the black hole's surface into E^3 is a visualization technique that does not alter the intrinsic geometry. As long as the embedding respects the isometry condition (preserving distances and curvatures), the derived relations are purely geometric and should remain valid regardless of the embedding choice. More specifically, embedding does not change the intrinsic Pythagorean relation; it simply provides a way to interpret or visualize it in a different geometric context. Furthermore, the independence of the Pythagorean relation is ensured for the following reasons:

(i) The Pythagorean relation emerges from the Smarr procedure, which is based on scalar invariants of Kerr-Newman black hole geometry.

(ii) The intrinsic geometry of the black hole surface is preserved under isometric embedding. Hence, the Pythagorean relation is not tied to a specific coordinate system or embedding choice. Instead, it reflects the Kerr-Newman black hole's deeper geometric and physical properties. The relation's appearance in the EKNBHGRS case is a manifestation of the black hole's unique symmetry and extremality. We conclude that EKNBHGRS is not merely a mathematical abstraction but a physically realizable solution within the Kerr-Newman black hole family, embodying a distinctive symmetry that aligns with the Smarr mass/energy framework.

6. Golden Ratio and Symmetry and Stability in Kerr-Newman-de Sitter Black Holes

Extremal black holes, with their uniquely balanced parameters of mass, charge, and angular momentum, occupy a threshold in black hole physics as they represent a state at the brink of naked singularity yet maintain thermodynamic stability by minimizing fluctuations in temperature and entropy. In [23–25], the authors analyzed extremal black holes and discussed the role of thermodynamic properties, such as entropy, in determining stability and insight into the concept of stable configurations. The discovery of a family of extremal Kerr–Newman black holes with fundamental quantities aligned to the golden ratio is relevant from the physical point of view, particularly when one member of this family uniquely satisfies the Pythagorean conditions at its umbilic points. This exceptional black hole, where all key physical properties - mass/energy, charge, angular momentum, and irreducible mass - align with the golden ratio, represents the pinnacle of symmetry achievable within the Kerr-Newman framework. This profound alignment, compatible with the constraints of the Kerr–Newman metric, hints at a unique state of equilibrium that may even offer a pathway to determine the dark energy density parameter for black holes in the Kerr-Newman-de Sitter geometry. In [26], the authors explored how the golden ratio

frequently arises in stable, self-organizing systems, setting a context for considering its application to complex systems like black holes. Assuming this special Kerr-Newman-de Sitter (KN-dS) black hole is in a state of marginal stability allows us to formulate a set of equations that may allow us to determine the dark energy density parameter, Ω_Λ. This parameter is defined as follows:

$$\Omega_\Lambda = \frac{\Lambda c^2}{3H^2} \tag{48}$$

with H denoting the Hubble constant. This formula provides Ω_Λ as the ratio of the cosmological constant's contribution to the total energy density of the universe, normalized by the critical density $\rho_{crit} = 3H^2/(8\pi G)$. Here is how each term contributes:

- The cosmological constant Λ represents a constant energy density uniformly filling space.
- The speed of light c is used to convert Λ (in units of inverse seconds squared $\sec^{-2}$) into energy density units.
- The Hubble constant H sets the current expansion rate of the universe and, thus, the critical density threshold.

This relation highlights the role of Λ in the overall energy content of the universe and how it drives cosmic acceleration in the context of the Λ-CDM model.

6.1. The Kerr-Newman-de Sitter (KN-dS) Metric

The Kerr-Newman-de Sitter (KN-dS) metric describes a black hole that has mass, charge, and angular momentum and exists within a spacetime that includes a cosmological constant Λ, representing a universe with a non-zero cosmological expansion. This metric generalizes the Kerr and Kerr-Newman solutions by incorporating the effects of Λ, allowing for an investigation of rotating and charged black holes within a cosmological setting (de Sitter or anti-de Sitter space, depending on the sign of Λ). The KN-dS metric is often given in Boyer–Lindquist coordinates (t, r, θ, ϕ) as follows:

$$ds^2 = -\frac{\Delta_r}{\rho^2}(dt - a\sin^2\theta d\phi)^2 + \frac{\rho^2}{\Delta_r}dr^2 + \frac{\rho^2}{\Delta_\theta}d\theta^2 + \frac{\Delta_\theta \sin^2\theta}{\rho^2}(adt - (r^2+a^2)d\phi)^2 \tag{49}$$

where

$$\rho^2 = r^2 + a^2\cos^2\theta \;\; ; \;\; \Delta_r = (r^2+a^2)\left(1 - \frac{\Lambda}{3}r^2\right) - 2mr + Q^2 \;\; ; \;\; \Delta_\theta = 1 + \frac{\Lambda}{3}a^2\cos^2\theta \tag{50}$$

The metric admits multiple horizons: a black hole event horizon, an inner Cauchy horizon, and a cosmological horizon if $\Lambda > 0$. The exact number and nature of these horizons depend on the values of m, Q, a, and Λ. As Λ increases, the cosmological horizon approaches the black hole event horizon, impacting the causal structure of the spacetime. Due to the black hole's rotation $(a \neq 0)$, the geometry is not spherically symmetric but rather axially symmetric. This creates frame-dragging effects where nearby particles are "dragged" along with the black hole's rotation. The electric charge Q adds an electromagnetic field around the black hole. For charged particles, this modifies the geodesics, particularly close to the black hole, where both gravitational and electromagnetic forces affect particle trajectories. The presence of the cosmological constant Λ impacts the geometry far from the black hole, leading to an asymptotically de Sitter (or anti-de Sitter if $\Lambda < 0$) structure. This influences the potential conformal boundary of the spacetime and the causal connectivity between regions. The KN-dS metric possesses killing vectors corresponding to time translation (∂_t) and rotational symmetry (∂_ϕ). However, unlike non-dS cases, the introduction of Λ changes the asymptotic structure from flat to de Sitter, affecting how these symmetries behave at large distances. In [1,27–29], we can find an analysis of the Kerr-de Sitter spacetime, providing insights that can be extended to the Kerr-Newman-de

Sitter case. In particular, in [30], the authors explored the effects of a cosmological constant on black hole horizons and thermodynamics, which applies directly to KN-dS black holes.

6.2. Calculating the Dark Energy Density Parameter under Marginal Stability

If we assume that the extremal Kerr-Newman black hole with golden ratio symmetry in the KN-dS setup is at marginal stability, we may potentially determine Ω_Λ (work to be submitted to review).

(i) The extremal conditions for Kerr–Newman black holes imply specific relationships between m, Q, L, and the irreducible mass, m_{ir}. Here, all these quantities are proportional to m_{ir} by factors involving the golden ratio, $-\phi_-$.
(ii) The unique condition where these quantities align with $-\phi_-$ suggests that the black hole's structure at the umbilic points is characterized by the golden ratio symmetry, potentially influencing the Gaussian curvature. This constrains Ω_Λ since the cosmological constant Λ would need to support this symmetry to maintain marginal stability.
(iii) The marginal stability assumption implies setting specific conditions on Ω_Λ, such that any additional increase would lead to instability. We could derive this using the equations for the KN-dS black hole horizons and matching them with the critical points where the golden ratio relations hold. This would involve solving the Einstein-Maxwell equations with Ω_Λ, subject to extremality and marginal stability conditions.
(iv) Solving these conditions should, in principle, yield an expression for Ω_Λ in terms of $-\phi_-$ and the other physical parameters (mass, charge, angular momentum) of the black hole.

The EKNBHGR's symmetry offers a natural framework for deriving the dark energy density Ω_Λ, linking black hole physics with cosmology. The presence of the golden ratio in the structure or stability of Kerr-Newman-de Sitter black holes, particularly in a family that adheres to golden ratio proportions, could imply that this symmetry is a marker of stability or "marginal stability" not just in black holes but in spacetime itself. It might indicate that certain cosmological properties, like the dark energy parameter Ω_Λ, are the "most stable" or "natural" configuration of the universe. Extremal black holes like EKNBHGRS can arise in specific cosmic scenarios, such as black hole mergers or high-energy events, making this configuration plausible within general relativity. To summarize, EKNBHGRS is a unique, physically grounded solution with significant implications for black hole thermodynamics, symmetry, and cosmology. It makes a meaningful contribution to both classical and quantum gravity research.

6.3. Thermodynamics of Kerr-Newman-de Sitter Black Holes

Thermodynamic stability claims specific calculations for quantities like specific heat and entropy fluctuations. This subject is extensively treated in the forthcoming manuscript [31]. The stability of a thermodynamic system under small variations of its coordinates can be assessed by examining the properties of its entropy S. Specifically, stability demands that the entropy hypersurface remains entirely beneath its corresponding tangent hyperplanes, implying that entropy must be a concave function of the system's extensive entropic parameters. This criterion imposes constraints on the system's physical observables. The stability conditions are analyzed by considering two cases: canonical ensemble and grand canonical ensemble. Without entering into details, we briefly summarize below the procedure adopted.

Canonical Ensemble

In the canonical ensemble, black holes are analyzed under the conditions of fixed temperature T, angular momentum L, and charge Q. The corresponding thermodynamic potential in this framework is the Helmholtz free energy. We examined the thermodynamics in this ensemble within the (T, L)-plane while keeping the charge constant. In this representation, extremal black hole solutions are confined to the ordinate axis ($T = 0$), while the half-plane where $T > 0$ corresponds to non-extremal solutions.

Grand Canonical Ensemble

In the grand canonical ensemble, the critical surfaces are identified by setting the determinant of the Hessian matrix of the Gibbs potential to zero (or, equivalently, to diverge). This condition leads to an equation that can be readily solved for the charge parameter Q. As mentioned, the underlying idea is that the extremal Kerr-Newman black hole with golden symmetry corresponds to the maximum symmetry compatible with the Kerr–Newman geometry. In the Kerr–Newman–de Sitter (KN-dS) metric, we assume that such a black hole is marginally stable. We then obtain five equations for the five unknowns m, Q, L, m_{ir}, and Ω_Λ. The five equations are as follows:

(1) The mass/energy formula in KN-dS geometry;
(2) The extremum condition for EKNBHGRS in KN-dS geometry;
(3) The condition for golden symmetry;
(4) The condition that ensures the Pythagorean relation between the fundamental forms is satisfied at the umbilical points;
(5a) The marginal stability of EKNBHGRS in the canonical ensemble.

or,

(5b) The marginal stability of EKNBHGRS in the grand canonical ensemble.

These five equations determine the solutions for the five variables m, L, Q, m_{ir}, and Ω_Λ, expressed entirely in terms of the golden ratio conjugate $(-\phi_-)$ (apart from the gravitational constant and the speed of light). It is important to note that in the above points (5a) and (5b), our primary focus is on identifying the regions where the system exhibits local stability. These regions are enclosed by critical hypersurfaces, where we have the following:

$$Det\left(\frac{\partial^2 S}{\partial X_i \partial X_j}\right) = 0 \tag{51}$$

where $X_i = m,\ L,\ Q$. Detailed calculations are underway.

7. Removal of Energy from an Extremal Kerr–Newman Black Hole by Reversible Transformations

We are now interested in calculating the energy extraction from the extreme black hole (9). As seen, the extreme Kerr–Newman geometry corresponds to the following:

$$m^2 = Q^2 + a^2 \tag{52}$$

From Equations (1) and (3), we obtain the following:

$$\begin{aligned} r_+ &= m \\ m_{ir} &= \frac{1}{2}\sqrt{m^2 + a^2} \end{aligned} \tag{53}$$

The mass/energy Formula (3) tells us that the energy of a Kerr–Newman black hole is given by three contributions [4]: (1) the *irreducible contribution to energy*, (2) the *electromagnetic contribution to the energy*, and (3) the *rotational contribution to the energy*. A black hole transformation that holds fixed the irreducible mass is *reversible*, and one that increases it is *irreversible* [11,32]. The removable energy from a black hole m_{extr} is clearly given by the following:

$$m_{extr} = m_{BH}^{(i)} - m_{BH}^{(f)} \tag{54}$$

with $m_{BH}^{(i)}$ and $m_{BH}^{(f)}$ denoting the black hole energy before and after the extraction, respectively. By removing all of the electromagnetic and rotational energy from the black hole through a reversible transformation (i.e., $m_{ir} = const.$), we obtain $m_{BH}^{(f)} = m_{ir}$. Hence, we have the following:

$$m_{extr} = m - m_{ir} \tag{55}$$

with $m = m_{BH}^{(i)}$ given by Equation (52). Our task is to determine the limit values of m_{extr}, i.e., $m_{extr}|_{min}$ and $m_{extr}|_{Max}$, for extreme Kerr–Newman black holes. Taking into account that $0 \leq \beta \leq 1/\sqrt{2}$, or $0 \leq a \leq \sqrt{2}m_{ir}$, from Equation (53), we obtain that the energy that can be extracted from an extreme Kerr–Newman black hole by a *reversible transformation* (i.e., $m_{ir} = const.$) is in the range of values

$$\left(1 - \frac{1}{\sqrt{2}}\right) m \leq m_{extr} < \frac{1}{2} m \qquad \text{i.e.,} \qquad 29.28\% \leq \frac{m_{extr}}{m} < 50\% \tag{56}$$

As previously mentioned, there are two geometrically distinct classes of Kerr–Newman black holes, as follows:

Class (a): $0 \leq \beta \leq 1/2$ or $0 \leq a \leq m_{ir}$
Class (b): $1/2 < \beta \leq 1/\sqrt{2}$ or $m_{ir} < a \leq \sqrt{2}m_{ir}$

7.1. Class (a)

This class consists of black holes with a positive Gaussian curvature. These black holes are oblately deformed spheres and they can be embedded in E^3. So, the range of extractable energy from this class of extreme Kerr–Newman black holes is as follows:

$$\left(1 - \frac{1}{\sqrt{3}}\right) m \leq m_{extr} < \frac{1}{2} m \qquad \text{i.e.,} \qquad 42.26\% \leq \frac{m_{extr}}{m} < 50\% \tag{57}$$

7.2. Class (b)

This class consists of black holes where there are regions of negative Gaussian curvature both on and around the axis of symmetry. The surface of these black holes resembles a hybrid sphere and pseudo-sphere. This class is non-empty only if the charge is small enough and such that $\beta > 1/2$ and $Q < \eta/\sqrt{2}$ [15]. In this case, the range of extractable energy from this class of extreme Kerr-Newman black holes is as follows:

$$\left(1 - \frac{1}{\sqrt{2}}\right) m \leq m_{extr} < \left(1 - \frac{1}{\sqrt{3}}\right) m \qquad \text{i.e.,} \qquad 29.28\% \leq \frac{m_{extr}}{m} < 42.26\% \tag{58}$$

7.3. Energy Extractable from Extreme Black Holes (15) and (17)

The energy we can extract from the black hole (15) by reversible transformation amounts to the following:

$$\frac{E_{extr}}{E_m} = \left(1 - \frac{1}{\sqrt{3}}\right) = 42.26\% \tag{59}$$

while the energy extractable from the black hole (17) by reversible transformations amounts to the following:

$$\frac{E_{extr}}{E_m} = \left(1 - \frac{(-\phi_-)^{1/2}}{\sqrt{2}}\right) = 44.41\% \tag{60}$$

In other words, *by reversible transformations, from the black hole (15), it is possible to extract only the minimum possible energy. Furthermore, regarding the percentage, the energy extractable from the black hole (17) is greater than that of the black hole (15), and amounts to* 88.82% *of the maximum value extractable from an extreme Kerr–Newman black hole.*

8. Conclusions

We analyzed extreme black holes in the Kerr-Newman geometry. By looking at the geometrical version of the equations of mass/energy for extreme Kerr–Newman black holes, we found two meaningful cases. The first black hole (15) corresponds to the case where the distortion parameter β has the limit value $\beta = 1/2$. Alongside this case, there is another even more surprising one: there exists a particular extreme black hole (17), where all its

fundamental physical quantities (i.e., its mass, its charge, its angular momentum, and the extractible energy from the black hole by reversible transformations) are incommensurable with the black hole's irreducible mass. All these constants are expressed in terms of the golden ratio numbers $-\phi_-$. These extreme black holes are studied in the Christodoulou diagram, and their topology has been investigated using the tools of differential geometry. The first black hole (15) corresponds to the limit case where the event horizon surface is flat at the poles. As for the second extreme black hole (17), we prove that if this black hole satisfies the Pythagorean fundamental form relation at the umbilic points, then both the *scale parameter* and the Gauss curvature of the surface at the pole are equal to the golden ratio numbers. Furthermore, at the poles, the mean curvature of the surface is equal to the square root of the golden ratio. In this case, the *scaled fundamental quantities* mass, charge, and angular momentum are equal to the square root of the golden section raised to odd integers. Successively, we computed the energy extractible from these extreme black holes by reversible transformations. We showed that, by keeping the irreducible mass constant to its initial value, the energy we can extract from the extreme black hole (17) amounts to 88.82% of the maximum value that can be extracted from an extreme Kerr–Newman black hole. The energy extractible from this extreme black hole is greater than the energy extractible from the black hole (15). It is the authors' opinion that a clearer understanding of the surface geometry of the extreme Kerr–Newman family of black holes will shed light on other problems in the physics of black holes and, more generally, allow insight into astrophysical processes. In Section 6, we asked whether the geometric properties found in this family of these extreme Kerr–Newman black holes have physical consequences. Extremal black holes like the extremal Kerr-Newman black hole with golden symmetry can arise in specific cosmic scenarios, such as black hole mergers or high-energy events, making this configuration plausible within general relativity. The idea of EKNBHGRS is quite intriguing, particularly in the context of an extreme Kerr-Newman black hole, where the golden ratio and Pythagorean conditions are satisfied at certain critical points known as umbilic points. This concept appears to explore deep connections between black hole physics, geometry, and black hole stability linked to the golden ratio. In this scenario, imposing marginal stability in the unique extremal Kerr–Newman–de Sitter black hole (a Kerr–Newman black hole with a cosmological constant, Λ) belonging to the family of the extremal Kerr–Newman black hole with golden ratio symmetry leads to the calculation of the dark energy density parameter Ω_Λ. Marginal stability typically refers to the condition where the system is on the verge of becoming unstable; in the context of black holes, this can relate to the balance between gravitational attraction, electromagnetic forces, and possibly repulsive effects from Λ. To calculate Ω_Λ under these conditions, one would need to balance the relevant physical parameters, particularly the mass m, charge Q, angular momentum L, and Λ, such that the black hole remains in a state of marginal stability while also satisfying the golden ratio condition at the umbilic points. Given the complexity of the Kerr–Newman–de Sitter metric, this involves solving the Einstein-Maxwell equations with a cosmological constant for the specific case where the golden ratio conditions are satisfied. This leads to a relationship between Ω_Λ and the other black hole parameters (m, Q, L) expressed in terms of the golden ratio $-\phi_-$. Detailed calculations are underway. Extremal black holes like EKNBHGRS can arise in specific cosmic scenarios, such as black hole mergers or high-energy events, making this configuration plausible within general relativity.

Author Contributions: Conceptualization, G.S.; methodology, G.S.; software, G.S. and P.N.; validation, G.S. and P.N.; formal analysis, G.S.; writing—original draft preparation, G.S.; writing—review and editing, G.S. and P.N.; visualization, G.S., supervision, G.S. and P.N. All authors have read and agreed to the published version of the manuscript.

Funding: This research received no external funding.

Data Availability Statement: Upon request, the authors can provide the Mathematica software codes used to perform the numerical calculations presented in this study.

Acknowledgments: GS expresses gratitude to Remo Ruffini for his warm welcome to the International Center for Relativistic Astrophysics Network (ICRANet) in Pescara, Italy, as well as the discussions. The authors also extend their gratitude to Philippe Peeters from the Université Libre de Bruxelles (ULB) for the valuable discussions and suggestions.

Conflicts of Interest: The authors declare no conflicts of interest.

Appendix A. Geometrical Interpretation of the Two Families of Extremal Black Holes

Equations (9)–(11) are geometrically equivalent to four interconnected right triangles. This can easily be verified by examining Figure A1.

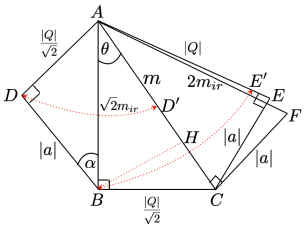

Figure A1. Geometrical version of the extreme Kerr–Newman black holes equations. The right triangle ABC and the right triangle ADB are the first and the second equations of System (9), respectively. Triangles ACE and ACF correspond to Equation (10) and Equation (11), respectively. Note that extreme Kerr–Newman black holes satisfy the relation $\sqrt{2}m_{ir}\sin\alpha = m\sin\theta$.

From Figure A1, we see that the two special cases (i) and (ii) investigated by us can be obtained by performing the rotations indicated with the red dotted arrows. More specifically,

Case (i)

This corresponds to the case where triangle ABC is the same as triangle ACE (see Figure A2).

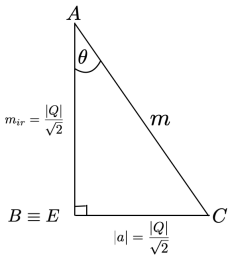

Figure A2. Special configuration (**i**): triangle ABC is exactly the same as triangle AEC.

Indeed, this condition implies the following:

$$|Q| = \frac{1}{\sqrt{2}}\eta \tag{A1}$$

So, from System (9), we obtain the following:

$$\begin{aligned} \bar{m} &= \sqrt{\frac{3}{2}}\eta \\ |Q| &= \frac{1}{\sqrt{2}}\eta \\ |\bar{L}| &= \frac{\sqrt{3}}{2}\eta^2 \end{aligned} \tag{A2}$$

Case (ii)

This corresponds to the case where one of the catheters of the right triangle ADB coincides exactly with the height of the triangle ABC relative to the base AC (see Figure A3).

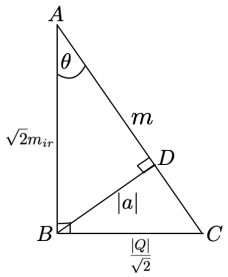

Figure A3. Special configuration (**ii**): the catheter BD of the right triangle ADB coincides exactly with the height of the triangle ABC relative to the base AC.

By imposing this condition for the catheter BD, we obtain the following:

$$|\bar{L}| = \eta |Q| \tag{A3}$$

which, combined with Equation (13), leads to the following:

$$\begin{aligned} \bar{m} &= (-\phi_-)^{-1/2}\eta \\ |Q| &= (-\phi_-)^{1/2}\eta \\ |\bar{L}| &= (-\phi_-)^{1/2}\eta^2 \end{aligned} \tag{A4}$$

where ϕ_- is one of the solutions to the golden ratio equation, as follows:

$$\phi^2 - \phi - 1 = 0 \tag{A5}$$

i.e.,

$$\phi_- = \frac{1-\sqrt{5}}{2} \tag{A6}$$

Appendix B. Determination of the First and the Second Fundamental Forms and Derivation of the Equation for the Umbilic Points

In these appendices, we shall demonstrate the theorems used throughout this work. There are three types of so-called fundamental forms. The most important are the first and second forms (since the third form can be expressed in terms of these). The first fundamental form (or line element) is given explicitly by the Riemannian metric, as follows [33]:

$$ds^2 = Edu^2 + 2Fdudv + Gdv^2 \tag{A7}$$

This form expresses the principal linear part of the growth of the arc length between two extremely close points located at the surface. The second fundamental form is given explicitly by the following:

$$ds^2 = Ldu^2 + 2Mdudv + Ndv^2 \tag{A8}$$

The second fundamental form is used to define the extrinsic invariants of a surface, such as its principal curvatures. It applies to a smooth submanifold that is immersed in a Riemannian manifold. If an arbitrary surface $\mathcal{S}$ is parametrized as

$$\mathcal{X} = (x(u,v), y(u,v), z(u,v)) \tag{A9}$$

then the matrices corresponding to the first and second fundamental forms $\mathcal{I}$ and $\mathcal{II}$ read, respectively, as follows:

$$\mathcal{I} = \begin{pmatrix} E & F \\ F & G \end{pmatrix} \qquad \mathcal{II} = \begin{pmatrix} Ł & M \\ M & N \end{pmatrix} \tag{A10}$$

where

$$E = (\mathcal{X}_u \cdot \mathcal{X}_u); \quad F = (\mathcal{X}_u \cdot \mathcal{X}_v); \quad G = (\mathcal{X}_v \cdot \mathcal{X}_v) \tag{A11}$$
$$Ł = (\mathcal{X}_{uu} \cdot \mathcal{N}); \quad M = (\mathcal{X}_{uv} \cdot \mathcal{N}); \quad N = (\mathcal{X}_{vv} \cdot \mathcal{N}) \quad \text{with}$$
$$\mathcal{N} = \frac{\epsilon(\mathcal{X}_u \wedge \mathcal{X}_v)}{|\mathcal{X}_u \wedge \mathcal{X}_v|} \quad \text{and} \quad W = (EG - F^2)^{1/2}$$

In Equation (A11), the subscript at the bottom of the variable indicates the *derivative of the variable with respect to that subscript*. Furthermore, $\epsilon = +1$ if the triple of vectors $\{\mathcal{X}_u, \mathcal{X}_v, \mathcal{N}\}$ has a right-hand orientation, and $\epsilon = -1$ in the opposite case. With metric (32), for an arbitrary surface of revolution in Euclidean 3-space (E^3) parametrized as follows:

$$\mathcal{X} = (f(v)\cos\theta, f(v)\sin\theta, g(v)) \tag{A12}$$

we obtain the following:

$$\mathcal{I} = \eta^2 \begin{pmatrix} h^{-1} & 0 \\ 0 & h \end{pmatrix} \qquad \mathcal{II} = \eta^{-2} \begin{pmatrix} f(g''f' - g'f'') & 0 \\ 0 & f^2 g' \end{pmatrix} \tag{A13}$$

The determinant of the ratio of the second (with respect to the first one) is the Gaussian curvature of the surface at the point [19], as follows:

$$K_G = \frac{ŁN - M^2}{W^2} \tag{A14}$$

This quantity measures the geometry intrinsic to the horizon itself and is independent of the embedding space. The trace of this ratio, i.e.,

$$H = \frac{EN + GŁ - 2FM}{2W^2} \tag{A15}$$

defines the mean curvature of the surface at the point [19]. The extrinsic curvature depends on the embedding space. As the parameter β varies, the shape of the black hole deforms, i.e., the extrinsic curvature varies while preserving the intrinsic geometry. With metric (32), we obtain the following:

$$K_G = \eta^{-2}\Big(1 - \beta^2(1+3\mu^2)\Big)\Big(1 - \beta^2(1-\mu^2)\Big)^{-3} \tag{A16}$$
$$H = \frac{1}{2}\eta^{-1}h^{-1/2}\Big(1 - \mu^2(1-\mu^2)^{-4}h^4\Big)^{1/2}\Big(1 - \mu^2(1-\mu^2)^{-4}h^4 + h_1\Big) \quad \text{with}$$
$$h = (1-\mu^2)\Big(1 - \beta^2(1-\mu^2)\Big)^{-1}$$
$$h_1 = \Big(1 - \beta^2(1+3\mu^2)\Big)(1-\mu^2)\Big(1 - \beta^2(1-\mu^2)\Big)^{-4}$$

The surface of a Kerr-Newman black hole can be globally embedded in E^3 if $\beta < 1/2$ and cannot be globally embedded in E^3 if $\beta > 1/2$ [15].

An umbilic point is a point on a surface at which the curvature is the same in any direction. In the differential geometry of surfaces in three dimensions, umbilic points are points on a surface that are locally spherical. At an umbilic, the first fundamental form $\mathcal{I}$ is proportional to the second fundamental form $\mathcal{II}$ [34]. Hence, we have the following:

$$Ł = \kappa E \quad \text{and} \quad N = \kappa G \quad \text{with} \quad \kappa = constant \tag{A17}$$

From Equation (A17), we have the following:

$$\frac{Ł}{N} = \frac{E}{G} \tag{A18}$$

From Equation (A13) we have the following:

$$\frac{Ł}{N} = h^{-2} \quad \text{or} \quad g'' f' - f'' g' = f g' (1-\mu^2)^{-2} \left(1 - \beta^2 (1-\mu^2)\right)^2 \tag{A19}$$

After using simple algebra, we finally obtain the equation for umbilic points as follows:

$$(1-\mu^2)\left(1-\beta^2\left(1+3\mu^2\right)\right) - \left(1-\beta^2\left(1-\mu^2\right)\right)^4 + \mu^2 = 0 \tag{A20}$$

Appendix C. Solution to the Pythagorean Fundamental Form Equation

In differential geometry, a surface immersed in 3-dimensional space is said to fulfill the *Pythagorean-like formula* if the following relation among the fundamental forms is satisfied:

$$\mathcal{I}^2 + \mathcal{II}^2 = \mathcal{III}^2 \tag{A21}$$

with $\mathcal{I}$, $\mathcal{II}$, and $\mathcal{III}$ denoting the matrices corresponding to the surface's first, second, and third fundamental forms, respectively [35]. In differential geometry, the third fundamental form is a surface metric that, unlike the second fundamental form, is independent of the surface normal. The third fundamental form is expressed in terms of the first and second fundamental forms, as described by [36]:

$$K_G \cdot \mathcal{I} - 2H \cdot \mathcal{II} + \mathcal{III} = 0 \tag{A22}$$

At the umbilic points, we have $Ł = \kappa E$ and $N = \kappa G$. Hence, at the umbilic points, the Gauss curvature of the surface and the mean curvature of the surface simply read as follows:

$$\begin{aligned} K_G &= \frac{ŁN - M^2}{W^2} = \frac{\kappa^2 EG}{EG} = \kappa^2 \\ H &= \frac{Ł G + NE - 2FM}{2W^2} = \frac{2\kappa EG}{2EG} = \kappa \end{aligned} \tag{A23}$$

At the umbilic points, the third fundamental form reads as follows:

$$\mathcal{III} \equiv \begin{pmatrix} P & 0 \\ 0 & Q \end{pmatrix} = 2H \begin{pmatrix} Ł & 0 \\ 0 & N \end{pmatrix} - K_G \begin{pmatrix} E & 0 \\ 0 & G \end{pmatrix} \tag{A24}$$

or

$$\mathcal{III} \equiv \begin{pmatrix} P & 0 \\ 0 & Q \end{pmatrix} = 2\kappa \begin{pmatrix} \kappa E & 0 \\ 0 & \kappa G \end{pmatrix} - \kappa^2 \begin{pmatrix} E & 0 \\ 0 & G \end{pmatrix} = \kappa^2 \begin{pmatrix} E & 0 \\ 0 & G \end{pmatrix} \tag{A25}$$

The horizon of a black hole satisfies the Pythagorean-like formula at the umbilic points if we have the following:

$$\kappa^4 \begin{pmatrix} E & 0 \\ 0 & G \end{pmatrix} = \kappa^2 \begin{pmatrix} E & 0 \\ 0 & G \end{pmatrix} + \begin{pmatrix} E & 0 \\ 0 & G \end{pmatrix} \tag{A26}$$

Equation (A26) is satisfied for all values of E and G if, and only if, the following equation is satisfied:

$$\kappa^4 - \kappa^2 - 1 = 0 \tag{A27}$$

The positive solution to Equation (A27) reads as follows:

$$\kappa^2 = \phi_+ \tag{A28}$$

Hence, we have the following:

$$K_G = \phi_+ \qquad \text{and} \qquad H = \phi_+^{1/2} \tag{A29}$$

The main result of our analysis is as follows: *If the extreme Kerr–Newman black hole (17) satisfies the Pythagorean-like formula at the umbilic points, then the horizon is locally metrically equivalent to a 2-sphere at these points, with the Gauss curvature of the surface equal to the golden ratio and the mean curvature equal to the square root of the golden ratio.*

References

1. Carter, B. Global Structure of the Kerr Family of Gravitational Fields. *Phys. Rev.* **1968**, *174*, 1559. [CrossRef]
2. Newman, E.; Couch, E.; Chinnapared, K.; Exton, A.; Prakash, A.; Torrence, R. Metric of a Rotating, Charged Mass. *J. Math. Phys.* **1965**, *6*, 918. [CrossRef]
3. Sonnino, G. Prigogine's second law and determination of the EUP and GUP parameters in small black hole thermodynamics. *Universe* **2024**, *10*, 390. [CrossRef]
4. Misner, C.W.; Thorne, K.S.; Wheeler, J.A. *Gravitation*; W. H. Freeman and Company: San Francisco, CA, USA, 1973.
5. Carter, B. Hamilton-Jacobi and Schrodinger separable solutions of Einstein's equations. *J. Math.Phys.* **1969**, *10*, 70. [CrossRef]
6. Bousso, R. The holographic principle. *Rev. Mod. Phys.* **2002**, *74*, 825. [CrossRef]
7. Burko, L.M.; Khanna, G.; Sabharwal, S. Linear stability of Schwarzschild singularities. *Phys. Rev. D* **2021**, *103*, L021502. [CrossRef]
8. Livio, M. *The Golden Ratio: The Story of Phi, the World's Most Astonishing Number*; Broadway Books: New York, NY, USA, 2002.
9. Ferrara, S.; Kallosh, R.; Strominger, A.N. Extremal Black Holes. *Phys. Rev. D* **1995**, *52*, R5412. [CrossRef]
10. Kallosh, R.; Linde, A. Supersymmetry and the Brane World. *J. High Energy Phys.* **2000**, *2*, 005. [CrossRef]
11. Christodoulou, D. Reversible and Irreversible Transformations in Black Hole Physics. *Phys. Rev. Lett.* **1970**, *25*, 1596. [CrossRef]
12. Christodoulou, D.; Ruffini, R. Reversible Transformations of a Charged Black Hole. *Phys. Rev. D* **1971**, *4*, 3552. [CrossRef]
13. Hawking, S. Gravitational Radiation from Colliding Black Holes. *Phys. Rev. Lett.* **1971**, *26*, 1344. [CrossRef]
14. Smarr, L. Mass Formula for Kerr Black Holes. *Phys. Rev. Lett.* **1973**, *30*, 71. [CrossRef]
15. Smarr, L. Surface Geometry of Charged Rotating Black Holes. *Phys. Rev. D* **1973**, *7*, 289. [CrossRef]
16. Sonnino, G. Surface Geometry of Some Meaningful Extremal Kerr-Newman Black Holes. *arXiv*. Available online: https://arxiv.org/pdf/2311.00665 (accessed on 14 March 2024).
17. Christodoulou, D. Investigations in Gravitational Collapse and the Physics of Black Holes. Doctoral Dissertation, Princeton University, Princeton, NJ, USA, 1971.
18. Klingenberg, W. *A Course in Differential Geometry*; Springer: Berlin/Heidelberg, Germany, 1978.
19. Spivak, M. A Comprehensive Introduction to Differential Geometry. Publish or Perish Inc., 1979. Hardcover. ISBN 10: 0914098837 ISBN 13: 9780914098836. Available online: https://www.abebooks.com/9780914098836/Comprehensive-Introduction-Differential-Geometry-Volume-0914098837/plp (accessed on 5 March 2024).
20. Pressley, A. *Elementary Differential Geometry*; Springer: London, UK, 2001.
21. Hitchin, N. Geometry of Surfaces—B3a Course 2013. Available online: https://people.maths.ox.ac.uk/joyce/Nairobi2019/Hitchin-GeometryOfSurfaces.pdf (accessed on 5 March 2013).
22. Aydin, M.E.; Mihai, A. A Note on Surfaces in Space Forms with Pythagorean Fundamental Forms *Mathematics* **2020**, *8*, 444. [CrossRef]
23. Hawking, S.W.; Horowitz, G.T. The Gravitational Hamiltonian, Action, Entropy, and Surface Terms. *Class. Quantum Gravity* **1996**, *13*, 1487. [CrossRef]
24. Gibbons, G.W.; Kallosh, R.E. Topology, Entropy, and Witten Index of Dilaton Black Holes. *Phys. Rev. D* **1995**, *51*, 2839. [CrossRef] [PubMed]
25. Carlip, S. Black Hole Thermodynamics. *Int. J. Mod. Phys. D* **2014**, *23*, 1430023. [CrossRef]
26. Spinadel, V.W. The Golden Ratio in Architecture, Art, and Nature. *Int. J. Math. Educ. Sci. Technol.* **1998**, *29*, 849.
27. Akcay, S.; Matzner, R.A. The Kerr-de Sitter universe. *Class. Quantum Gravity* **2011**, *28*, 085012. [CrossRef]
28. Griffiths, J.B.; Podolský, J. *Exact Space-Times in Einstein's General Relativity*; Cambridge University Press: Cambridge, UK, 2009.
29. Lake, K. Rotating de Sitter space-times. *Phys. Rev. D* **1974**, *19*, 2847. [CrossRef]
30. Gibbons, G.W.; Hawking, S.W. Cosmological event horizons, thermodynamics, and particle creation. *Phys. Rev. D* **1977**, *15*, 2738. [CrossRef]

31. Sonnino, G. Dark Energy Density from Extreme Black Holes at the Golden Ratio Limit. *arXiv* **2024**, arXiv:2311.00665v3. to be submitted for publication.
32. Bardeen, J.M.; Carter, B.; Hawking, S.W. The Four Laws of Black Hole Mechanics. *Commun. Math. Phys.* **1973**, *31*, 161. [CrossRef]
33. Weisstein, E.W. *Fundamental Forms*. From MathWorld—A Wolfram Web Resource. Available online: https://mathworld.wolfram.com/FundamentalForms.html (accessed on 16 August 2011).
34. MIT Education. Lines of Curvature Near Umbilics. Available online: https://web.mit.edu/hyperbook/Patrikalakis-Maekawa-Cho/node184.html (accessed on 1 December 2009).
35. Aydın, M.E.; Mihai, A.; Özgür, C. Pythagorean Isoparametric Hypersurfaces in Riemannian and Lorentzian Space Forms. *Axioms* **2022**, *11*, 59. [CrossRef]
36. Chase, H. Fundamental Forms of Surfaces and the Gauss-Bonnet Theorem. University of Chicago. Available online: https://api.semanticscholar.org/CorpusID:10726084 (accessed on 24 September 2014).